Applied Geochemistry 84 (2017) 13–25

Contents lists available at ScienceDirect

Applied Geochemistry

journal homepage: www.elsevier.com/locate/apgeochem

Geochemical constraints on the sources of Cr(VI) contamination in waters of Messapia (Central Evia) Basin

M. Economou-Eliopoulos [a, *], I. Megremi [a], Ch. Vasilatos [a], R. Frei [b], I. Mpourodimos [c]

[a] Department of Geology and Geoenvironment, University of Athens, Athens 15784, Greece
[b] Department of Geoscience and Natural Resource Management, University of Copenhagen, Denmark
[c] The Municipality of Messapia-Dirfis, Evia, Greece

ARTICLE INFO

Article history:
Received 10 May 2017
Accepted 11 May 2017
Available online 13 May 2017

Editorial Handling by Prof. M. Kersten.

Keywords:
Contamination
Cr(VI)
Water
Leachates
Isotopes
Evia

ABSTRACT

The present study aims to define geochemical constraints on contamination source(s) by Cr(VI) in Central Evia, through a compilation of new and literature data on an integrated set of approaches, including mineralogy and (isotope) geochemistry; leach experiments on rocks, soils and Ni-laterites; and comparison with literature data on groundwater.

The concentrations of Cr(VI) in leachates from various geological materials decrease in the following order: Ni laterites from Kastoria > soils > altered ultramafic rocks > Ni laterites from Evia. A salient feature is the diversity in the Cr(VI) concentrations and δ^{53}Cr values in (a) groundwater, ranging from <2 to 850 μg/L Cr(VI) and 0.60−1.99‰ δ^{53}Cr, and (b) leachates from Ni-laterites, ranging from 0.6 to 2.0 μg/L and 1.01‰ in Evia samples and from 750 to 1200 μg/L and negative to slightly positive (−0.21 to 0.03‰) δ^{53}Cr in Kastoria samples. A positive correlation ($R^2 = 0.514$) between the δ^{53}Cr values and depth of the aquifers, potentially reflects the decrease in soluble O_2 with increasing depth. The relatively high Cr, Mn and the abundance of fine-grained Mn-(hydr)oxides in the Kastoria laterite ore, may be major controlling factors for the existence of high Cr(VI) concentrations in the water leachates. In contrast, the low Cr(VI) concentrations and positively fractionated Cr isotopes in the Ni-laterite leachates from Evia are potentially related to redox and multistage transportation/redeposition processes.

The positive correlation between Cr concentrations and Ca/Mg ratios ($R^2 = 0.647$) for rock leachates and the negative correlation ($R^2 = -0.694$) for soil leachates suggest that Cr in groundwater may be released mainly from Cr-bearing Mg-silicates in altered ultramafic rocks and soils. The plot of δ^{53}Cr values *versus* Cr(VI) concentrations for the contaminated waters from Central Evia and Assopos Basin fall within both fields defined from a global database for natural waters and waters contaminated by human activities.

1. Introduction

Chromium occurs in different oxidation states in nature, with Cr(III) and Cr(VI) being the most abundant species. Cr(III) is a required nutrient, as opposed to the highly toxic and very soluble oxidized Cr(VI), which causes serious health problems (Kabata-Pendias, 2000) when in the form of chromate oxyanions such as CrO_4^{2-}, $HCrO_4^-$ and $Cr_2O_7^{2-}$ (ATSDR, 2000; Losi et al., 1994). Council Directive 98/83/EC has established a maximum permissible limit of Cr_{total} in drinking water, 50 μg/L or ppb. Chromium is used in many industrial processes, including iron and steel production, chrome plating, manufacture of pigments, leather tanning, and wood processing, and it may also be released by natural processes from Cr-bearing minerals hosted in rocks and ores such as ultramafic rocks and Ni-laterites. Chromium oxidation-reduction processes in natural waters and soil environments have long been an attractive topic for intense research (Salunkhe et al., 1998; Fantoni et al., 2002; Oze, 2003; Becquer et al., 2003; Ball and Izbicki, 2004; Oze et al., 2004, 2007, 2016). Recently, high concentrations (up to 120 μg/L) of Cr(VI) were determined in unconfined aquifers of the Sarigkiol Basin (Kozani area, N. Greece), effected by Ophiolitic rocks and fly ash produced from a power plant burning lignite (Kazakis et al., 2017).

Our research interest has focused on the Assopos – Thiva Basin because it is an industrial zone; the Assopos River running through the basin has been designated as a “processed industrial waste

* Corresponding author.
E-mail address: econom@geol.uoa.gr (M. Economou-Eliopoulos).

http://dx.doi.org/10.1016/j.apgeochem.2017.05.015
0883-2927/

receiver" since 1969 (Giannoulopoulos, 2008; Vasilatos et al., 2008; Tziritis, 2009; Megremi, 2009, 2010; Megremi et al., 2013; Economou-Eliopoulos et al., 2011, 2012, 2013, 2014, 2016; Frei and Polat, 2012, Frei et al., 2014a,b; Dermatas et al., 2015; Dimitroula et al., 2015; Dokou et al., 2015). The Central Euboea Basin (Messapia) has been selected for geological and environmental studies, due to the presence of widespread masses of ophiolitic rocks and Ni-laterite deposits, such as the Psachna Ni-laterite deposits in Evia, Larymna and Kastoria (Valeton et al., 1987; Skarpelis et al., 1993; Alevizos, 1997; Eliopoulos and Economou-Eliopoulos, 2000; Skarpelis, 1997; Megremi, 2009, 2010; Kalatha and Economou-Eliopoulos, 2015; Gkoutzioupa et al., 2016).

Given population growth, the need for production of more food, and the desire to avoid further losses in ecosystem biodiversity, soil and groundwater protection is of particular significance for societies and agricultural economies. The range and average Cr content in the Assopos Basin (range: 73–300 ppm, average: 200 ppm) and in the Central Evia soils (range: 540–3800 ppm, average: 1300 ppm) (Fig. 1) are often higher than the average Cr content in the earth's crust (80 ppm), although levels in the Assopos Basin do not always indicate contamination, according to metal limits (380 ppm) given for soils by the Netherlands (Kabata-Pendias, 2000). Concentrations of Cr(VI) in groundwater above the acceptable level are common in the Assopos Basin, ranging from <2 to 900 μg/L, and the Central Evia, ranging from <2 to 350 μg/L (Megremi, 2009, 2010; Economou-Eliopoulos et al., 2012, 2014, 2016).

The present review study is a compilation of new and literature data from a variety of topical studies, including mineralogy, (isotope) geochemistry, and leaching experiments on rocks, soils and Fe-Ni-laterites from Central Evia (Messapia). This database is compared to that of other contaminated groundwater and leachates, in an attempt to define mineralogical and geochemical constraints on the source(s) of contamination.

2. Geological and hydrogeologic outline

The regional aquifer is a complex heterogeneous system in the area of central Euboea, composed mainly of alluvial Neogene sediments and ultramafic rocks. The shallow portion of the regional aquifer is predominantly under phreatic (unconfined) conditions, has limited thickness (less than 100 m), and is commonly used for agricultural activities. Ophiolitic outcrops, consisting mainly of serpentinized peridotites (harzburgites and lherzolites) with some minor mafic rocks, are common. The area is characterized by strong geomorphological contrast and consists mainly of Pleistocene to Holocene sediments, which host the most productive aquifers in this area (Fig. 1; Katsikatsos et al., 1980). Central Evia, aside from the Quaternary alluvial formations and ophiolites covering lowland areas, is characterized by widespread Ni-laterite deposits. The Ni-laterite deposits in Central Evia, in the proximity of the studied area, as well as those in Larymna, Central Greece, are well-known due to a production level corresponding to approximately 2–3% of the world's total nickel output (Megremi, 2010; Eliopoulos et al., 2012). Ni-laterite ores have been transported and deposited either onto peridotites or onto karstified Jurassic limestone and overlain by Lower Cretaceous limestone. The multistage transportation and redeposition of the latter deposits is well-documented by the

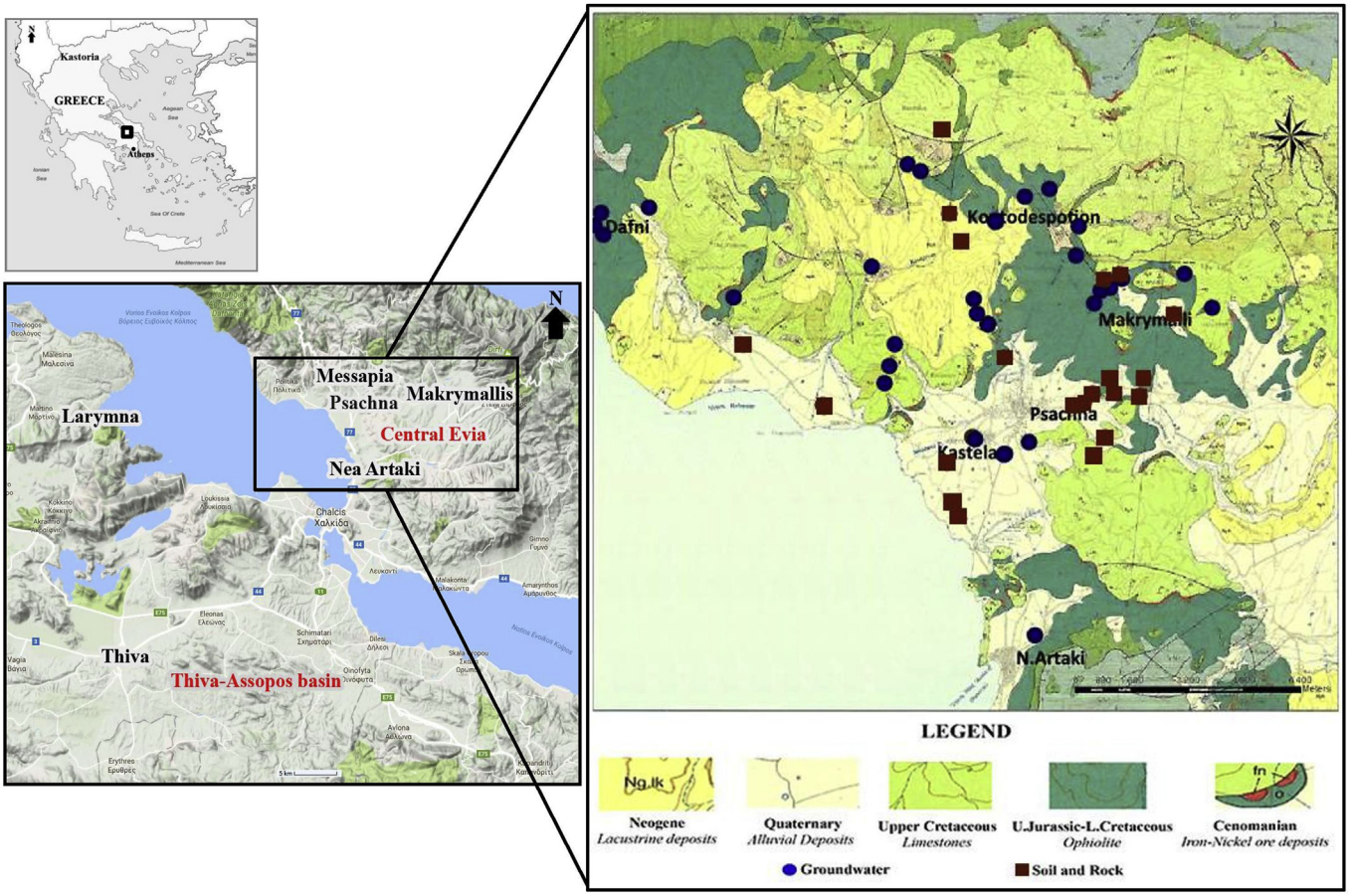

Fig. 1. Geological map showing the sampling location in Central Evia.

presence of a conglomerate, composed mostly of rounded-elongated saprolite and silicified saprolite blocks (of varying size) within a matrix of pisolitic laterite and calcite, at the contact between the laterite body and the carbonate basement (Alevizos, 1997; Skarpelis, 1997; Eliopoulos and Economou-Eliopoulos, 2000; Kalatha and Economou-Eliopoulos, 2015; Valeton et al., 1987).

Thus, two different types of aquifers can be found: (a) Neogene aquifers in conglomerates, sandstones and marly limestone, and/or in highly fractured zones of ultramafic rocks (harzburgites and lherzolites), reaching depths between 11 and 180 m, which are tapped by many shallow wells for agricultural activities, and (b) a deeper karst-type aquifer associated with Jurassic-Cretaceous limestones. The deep portion of the regional aquifer is predominantly under confined conditions, and it appears that the hydraulic connection between the phreatic zone and deeper parts of the aquifer is poor (Katsikatsos et al., 1980; Megremi, 2010).

3. Methods of investigation

More than 60 soil samples were collected from cultivated and non-cultivated sites of Central Evia, covering an area of approximately 200 km^2 (19 km × 12 km). Soil samples, along with 25 rock and ore samples, collected between 2007 and 2012, have been analysed by inductively coupled plasma mass spectroscopy (ICP/MS), the soils after hot aqua regia digestion, and rock/ores after multi-acid digestion (HNO_3—$HClO_4$—HF—HCl), at ACME Analytical Laboratories in Canada. Detection limits and the results for the quality control samples, the precision of the analyses of the minor and trace elements is in good agreement with international standards (Table 1 in the Annex after Megremi, 2009, 2010; Economou-Eliopoulos et al., 2014, 2016).

Polished sections prepared from rock, soil and Fe-Ni-laterite ores from Evia and Kastoria (Greece) were carbon coated and examined by reflected light microscopy and scanning electron microscope (SEM) with energy-dispersive spectroscopy (EDS). SEM-EDS analyses were carried out at the University of Athens Department of Geology and Geoenvironment using a JEOL JSM 5600 scanning electron microscope, equipped with automated energy-dispersive analysis system ISIS 300 OXFORD, with the following operating conditions: accelerating voltage 20 kV, beam current 0.5 nA, time of measurement 50 s and beam diameter 1–2 μm (Tables 2 and 3).

Groundwater samples collected from over 40 domestic and

Table 1
Major and trace element contents in ultramafic rock, soils, Fe-Ni laterites from Central Evia (Messapia) and Kastoria.

Rocks	mg L^{-1}							wt%			
	Cr	Mn	Ni	Co	Zn	Sr	V	Fe	Al	Mg	Ca
R1	1180	1900	940	82	39	13	45	4.0	1.3	11.3	10.6
R2	840	1180	940	44	48	19	53	3.8	3.1	9.8	10.4
R2a	2100	1120	1340	110	39	16	57	6.2	1.3	6.7	12.2
R3	1340	1040	1730	85	28	17	22	4.4	0.6	3.8	20.9
R4	1620	900	1510	74	43	59	37	4.0	0.8	11.4	12.2
R5	1660	740	1730	87	39	13	41	5.0	0.7	18.2	4.6
R6	1660	680	2000	90	50	4	57	5.8	0.8	21.2	0.7
R7	1050	610	1650	84	25	5	53	5.2	0.5	19.1	2.6
R8	1020	640	1520	77	29	105	45	4.3	0.9	18.7	3.6
R9	1320	790	2120	100	53	5	41	5.5	0.7	22.2	0.2
R10	1250	680	1770	80	38	6	38	5.5	0.5	21.3	1.6
R11	160	340	1810	66	17	67	2	2.7	0.0	12.6	11.7
R12	860	540	2300	93	23	65	4	3.9	0.0	17.8	5.7
R13	520	600	2030	95	22	21	9	4.2	0.1	19.3	5.4
R14	320	520	1640	76	18	70	7	3.3	0.1	12.3	15.3
R15	1000	650	2090	100	30	7	30	5.7	0.3	20.2	1.7
R17	1140	530	1490	74	26	20	25	3.7	0.5	9.8	15.4
R18	1720	660	1850	95	37	6	33	5.2	0.4	17.0	7.0
Soils											
S1	670	760	610	42	61	80	61	3.7	3.9	2.8	6.2
S2	930	1050	930	60	83	64	77	5.3	4.7	4.3	3.2
S3	2100	1180	2260	120	83	20	55	7.7	2.3	13.8	0.6
S4	1050	1080	1190	72	99	58	76	5.9	4.1	6.2	3.1
S5	880	780	780	52	73	76	67	4.3	4.1	3.7	6.1
S6	2100	1200	2200	120	96	40	61	8.5	2.7	10.8	1.8
S7	1340	790	1460	80	79	49	56	6.0	3.2	7.8	3.2
S8	1760	1130	2220	120	84	28	59	8.6	2.9	10.8	0.9
S9	1790	690	2300	110	71	21	46	8.1	2.0	14.8	0.6
S10	3350	1360	3050	160	96	22	74	11.6	2.4	10.8	0.8
S13	2000	1130	2560	130	70	19	44	8.2	1.3	14.8	0.3
S14	1380	990	1830	97	69	28	74	6.8	3.6	6.2	7.9
S16	2300	980	2100	97	70	28	51	7.3	1.8	13.4	1.9
Fe-Ni laterites											
Evia											
La18	7300	1000	7500	260	31	20	105	36.5	17.2	0.3	0.3
La12	4450	800	4400	250	25	21	110	33.2	5.2	0.7	0.4
La15	3200	1100	6700	180	51	29	150	37.1	5.9	2.1	1.8
La1	3700	1600	3000	210	10	30	100	30.5	5.3	0./7	0.2
Kastoria											
Kast-4	19500	7130	9500	1400	300	30	130	32.7	0.9	1.4	2.1
Kast-7	23000	6300	6300	420	400	25	140	45.5	0.9	0.8	0.6
Det. Limit	1	1	0.1	0.2	1	1	1	0.01	0.01	0.01	0.01
STD	200	1061	144	43	111	380	155	7.37	7.67	3.97	5.65

Table 2
Representative SEM-EDS analyses of Fe-Mn (hydr)oxides from Fe-Ni laterite deposits.

Central Evia										
Goethite (Fig. 2e)										
wt.%	Light grey				Dark grey					
SiO_2	6.2	5.8	2.8	5.7	12.9	7.1	7.3	0.5	n.d.	n.d.
Al_2O_3	1.9	4.9	3.3	5.1	4.6	7.2	8.3	19.6	40.2	39.9
Cr_2O_3	0.4	0.3	0.4	0.3	0.6	0.5	0.4	0.9	0.6	0.3
Fe_2O_3	74.1	72.75	77.7	72.8	66.2	69.8	67.6	64.1	44.5	43.8
TiO_2	n.d.	1.4	1.9	1.3	n.d.	1.6	1.7	1.5	1.3	1.7
MgO	1.2	n.d.	n.d.	0.3	0.9	0.3	n.d.	n.d.	n.d.	n.d.
CaO	0.4	0.3	n.d.	n.d.	n.d.	n.d.	n.d.	n.d.	n.d.	n.d.
MnO	0.4	0.4	0.6	0.4	n.d.	n.d.	0.4	n.d.	0.3	0.3
NiO	0.9	0.4	n.d.	0.4	0.7	0.4	0.3	0.8	n.d.	0.4
Total	85.5	86.25	86.7	86.3	85.9	86.9	86	87.4	86.9	86.4

Kastoria										
Goethite (Fig. 3)										
wt.%	Fig. 3a		Fig. 3b		Fig. 3d		Fig. 3e	Fig. 3f	Fig. 3d	
	Light grey						Dark grey	White	White	Veinlets
SiO_2	4.4	1.5	1.5	1.8	1.6	1.5	5.7	1.9	2.1	3.9
Al_2O_3	1.4	2.1	2.1	2.1	2.1	2.9	0.8	n.d.	n.d.	1.3
Cr_2O_3	0.6	2.1	2.1	3.4	1.6	4.2	0.5	n.d.	n.d.	n.d.
Fe_2O_3	73.3	76.1	76.2	75.1	76.9	74.3	70.8	93.3	92.9	35.3
TiO_2	n.d.	n.d.	n.d.	n.d.	n.d.	n.d.	n.d.	n.d.	n.d.	n.d.
MgO	0.9	0.6	0.6	0.7	0.6	n.d.	0.7	0.7	0.8	4.1
CaO	0.4	0.3	0.3	0.2	n.d.	n.d.	0.4	n.d.	n.d.	0.4
MnO	3.2	1.8	1.6	0.7	1.6	1.5	4.6	2.4	2.8	33.1
NiO	2.3	0.7	0.7	1.3	0.7	0.7	2.6	1.5	0.8	7.1
Total	86.5	85.2	85.1	85.3	85.1	85.1	86.1	99.8	99.4	85.2

Symbol: n.d. = not detected.

irrigation wells covering the area studied (2007–2013) have been analysed by ICP/MS at ACME Analytical Laboratories in Canada (Table 4 in the Annex; Economou-Eliopoulos et al., 2014, 2016).

A series of natural water leaching experiments were carried out to understand the impact of environmental conditions on the leaching of Cr(VI) at varying time, and selected samples with a significant Cr(VI) concentration to determine chromium isotopes. More specifically, numerous of rock and soil samples subjected to leaching tests, following those used currently (ATSDR, 2014) for hours, days and weeks, at a 10:1 water to solid ratio. Thus, 10 g of soil and/or rock sample and 100 ml of natural water were transferred into a 200 ml Erlenmeyer flask at room temperature, to study the long-term leaching responses of Cr under atmospheric conditions (Table 5 in the Annex after Economou-Eliopoulos et al., 2014, 2016).

Table 3
Representative SEM-EDS analyses of chromite from the Kastoria Fe-Ni-laterite deposit.

wt%	I-4.1	I-4.2	I-4.3	I-4.4	I-7.1	I-7.2	I-7.3	I-7.4	I-7.5	I-7.6
Al_2O_3	8.1	9.7	11.1	11.3	8.9	8.1	10.7	13.2	9.1	9.3
Cr_2O_3	61.4	60.7	57.5	58.5	58.4	59.6	58.8	57.3	59.8	59.4
Fe_2O_3	2.3	0.3	2.1	0.3	3.3	2.8	0.3	0.5	0.6	0.9
FeO	18.9	17.2	17.2	20.2	19.4	9.9	14.8	16.6	19.8	18.9
MgO	9.1	8.9	9.9	7.9	8.3	8.9	7.1	9.9	7.1	6.4
MnO	0.3	n.d.	0.9	0.5	1.1	1.3	0.3	2.1	2.1	4.9
CoO	0.3	2.3	n.d.	0.9	n.d.	9.1	7.8	n.d.	0.3	0.3
Total	100.4	99.1	98.7	99.6	99.4	99.7	99.8	99.6	98.8	100.1
Cr#	0.83	0.81	0.78	0.78	0.81	0.83	0.79	0.75	0.82	0.8
Mg#	0.54	0.52	0.51	0.42	0.43	0.61	0.47	0.52	0.4	0.41

Symbols: Cr# = Cr/(Cr + Al), Mg# = Mg/(Mg + Fe^{2+}).

Table 4
Trace element concentrations in groundwater from central Evia.

	µg/L					mg/L				
	Crtotal	Cr(VI)	As	B	Li	Ca	Mg	Na	Si	S
E1	33	32	0.9	30	2.7	39	50	22	13	15
E2	130	128	0.7	150	6.8	18	81	73	20	41
E3	53	51	0.8	40	4.1	32	76	38	17	29
E4	60	59	0.8	35	4	33	74	38	16	28
E5	114	110	0.9	60	5.8	64	103	40	17	68
E6	70	68	1.4	70	6.8	16	114	53	24	27
E7	360	360	0.7	40	7.3	64	13	32	28	44
E8	70	64	2	80	16	64	16	98	20	58
E9	86	83	1.3	50	11	59	89	44	19	32
E10	105	104	0.6	35	4.6	64	115	38	15	52
E11	68	63	1.6	36	6.3	114	87	39	13	57
E12	75	62	1.7	30	5.6	75	56	25	13	13
E13	56	56	1.4	90	9.1	142	134	79	13	110
E14	16	16	0.5	25	2.4	15	59	16	24	7
E15	25	25	0.7	20	3.8	20	52	20	24	6
E16	18	18	<0.5	10	0.2	35	28	12	10	3
E17	37	36	0.5	20	4.3	7	67	21	33	1
E18	33	32	<0.5	20	1	9	45	19	20	19
E19	32	32	<0.5	20	2	10	45	19	19	17
E20	16	12	<0.5	25	2.7	99	52	22	23	29
E21	13	12	<0.5	22	2.1	122	29	19	14	13
E22	52	51	<0.5	30	3.5	78	83	30	28	35
E23	15	15	2.6	15	1.6	9	80	15	34	8
E24	14	14	1.5	16	2.3	18	81	35	34	13
E25	37	36	0.5	20	4.5	9	68	22	32	1
E26	31	30	<0.5	23	3.7	49	74	22	31	5
E27	33	32	<0.5	23	3.4	48	74	19	30	4
E28	27	26	<0.5	17	1.9	94	43	23	21	19
E29	26	25	<0.5	17	2.7	65	70	22	26	5
E30	18	18	0.5	20	1.6	37	27	15	15	6
E31	17	12	<0.5	24	1.6	113	26	16	14	5
E32	15	14	<0.5	26	2.1	68	56	16	24	7
E33	<2	<2	<0.5	10	1.4	98	5	12	4	5
E34	<2	<2	0.6	13	0.7	46	8	14	6	6
E35	2	2	0.7	10	2.2	73	11	15	7	5
E36	3	3	<0.5	11	0.9	44	10	14	6	5
E37	<2	<2	0.5	8	1	51	4	12	4	4
E38	5	4	<0.5	10	0.7	118	13	11	7	4
E39	22	20	1.8	24	3.7	85	42	65	8	13
E40	23	20	2	23	3.5	85	43	66	8	11
E41	23	19	2	23	3.7	86	44	66	8	12

High-precision stable chromium isotopes (expressed as $\delta^{53}Cr$ values) have been measured in groundwater and in water leachates of ultramafic rocks, soils and Fe-Ni-laterite ores (Economou-Eliopoulos et al., 2014, 2016) on a multi-collector inductively coupled plasma source mass spectrometry (MC–ICP–MS) (Schoenberg et al., 2008; Schiller et al., 2014). The final isotopic composition of a sample (Table 6) was determined as the average of the repeated analyses and reported relative to the certified SRM 979 standard as

$$\delta^{53}Cr(\%) = \left[\left({}^{53}Cr/{}^{52}Cr_{sample}/{}^{53}Cr/{}^{53}Cr_{SRM979}\right) - 1\right] \times 100.$$

4. Results and selected characteristics of rocks, soils and ores

The occurrence of highly serpentinized and tectonized rocks and the multistage transportation and re-deposition of the Fe-Ni laterite deposits is in Central Evia and Lokris are well documented by the presence of a conglomerate, composed mostly of rounded-elongated saprolite and silicified saprolite blocks (of varying size) within a matrix of pisolitic laterite and calcite, at the contact between the laterite body and the carbonate basement (Fig. 2a–d). Soil, rock and Fe-Ni-laterite samples from Central Evia

Table 5
Trace element concentrations in leachates from peridotites, soils and Fe-Ni laterites from C. Evia and Kastoria (Kast).

	μm/L										mg/l				
	Crtotal	Cr(VI)	As	B	Br	Li	Mn	Ni	P	Zn	Ca	Mg	Na	Si	S
Rock leachates															
R1	14	12	0.5	268	7	1.4	0.2	7	<10	9.1	27	2.1	3.2	13	<1
R2	18	16	1.6	154	13	2.7	0.1	4.2	11	4	26	1.9	4.2	12	<1
R2a	35	35	1.7	124	<5	3.2	0.2	2.3	<10	5.5	26	1.9	3.4	12	<1
R3	30	29	0.8	78	<5	14.8	0.5	0.7	<10	6.1	25	2.9	2.4	13	<1
R4	3	<4	0.6	46	<5	3.4	0.1	0.7	<10	6.9	18	4.7	2.1	15	<1
R5	3.2	<4	0.5	23	<5	1.6	0.7	1.1	<10	6	18	6.8	1.9	17	<1
R6	2	<4	<0.5	103	12	1	0.1	0.7	<10	3.5	12	11.4	3.3	18	<1
R7	2.3	<4	0.6	204	<5	1.4	<0.05	0.9	<10	3.7	13	11.8	1.9	23	<1
R8	2.2	<4	0.7	106	<5	0.8	0.2	0.8	<10	8.2	13	8.6	1.8	20	<1
R10	3.1	<4	<0.5	272	5	0.5	0.2	0.2	<10	4.7	15	11.6	1.7	26	<1
R11	4.8	4.5	<0.5	46	11	0.5	0.5	0.4	<10	29	25	8.1	1.5	33	<1
R13	3.4	<4	<0.5	148	<5	0.4	<0.05	<0.2	<10	<0.5	12	13.8	1.6	23	<1
R15	6.4	5	<0.5	143	13	0.6	<0.05	0.7	<10	1.8	16	11.3	2.3	22	<1
R16	5.5	4	<0.5	58	18	0.9	<0.05	<0.2	<10	0.5	20	13.2	2.1	19	<1
R17	3.6	<4	<0.5	229	<5	1.6	<0.05	0.6	<10	1.9	18	6.3	2.1	17	<1
R18	8.8	7	<0.5	48	<5	0.5	<0.05	0.4	<10	1.6	21	8.1	1.7	17	<1
R19	15	13	<0.5	292	27	0.9	0.1	0.7	<10	5.8	20	6.8	4	20	<1
Soil leachates															
S1	21	17	4.9	2811	52	5.5	0.2	10	38	7.8	30	11.7	7.5	17	2
S2	27	21	11	5417	54	7.3	0.2	15	1040	5	26	15.9	10.1	20	1
S3	94	87	5.2	930	24	2.9	0.2	32	874	9.8	13	17.4	4.1	22	<1
S4	38	34	10	1233	36	4.4	0.2	21	2124	1.3	20	18.7	5.9	14	1
S5	37	28	4.6	1412	27	4.5	0.2	9	120	3.8	34	6.8	4.1	13	1
S6	76	68	5.6	767	31	2.3	0.3	28	1236	4.1	25	12.8	4.4	17	3
S7	35	35	12	254	45	3.1	0.1	25	747	4.2	29	12.1	4.7	14	2
S8	64	43	3.4	253	26	2.7	0.5	39	746	43.5	26	21.4	3.6	21	3
S9	57	43	4.6	248	43	4	0.1	22	972	1.8	20	15.7	4.6	21	1
S19	58	76	2.7	620	49	3	0.1	13	214	5.5	26	8.4	3.9	17	<1
S11	84	81	2.9	1019	35	2.7	0.1	17	463	7.6	32	6.1	3.4	12	1
S13	70	48	1.6	286	24	3.7	0.4	54	756	19	16	14.2	3.9	18	2
S14	22	18	2.1	511	34	1.8	0.2	24	38	9.6	44	4.6	2.3	11	1
S16	58	55	2.3	740	18	2.4	0.1	13	360	<0.5	29	14	3.4	18	<1
Fe-Ni laterites															
La18	1.8	2	1.4	11,400	170	55.5	170	12	57	1.3	26	24	19	9	5
La12	1.3	1.3	<0.5	1960	21	6.4	1.1	5.6	<10	4	31	8.9	8.9	7	4
La15	0.57	0.6	1.8	1620	20	11.4	0.6	3.6	<10	4.6	26	1	9.7	7	4
La1	0.74	0.8	0.9	600	17	4.9	1.5	2.8	<10	8.3	46	18	15	7	6
Kast4	1200	1300	<0.5	21,700	70	7.2	0.22	9.4	<10	0.4	29	4.3	24	31	5
Kast7	750	740	<0.5	8900	82	3.7	0.6	3.6	<10	0.5	43	1.4	16	7.5	5
D. Limit	0.5		0.5	5	5	0.1	0.1	0.2	10	0.5	0	0	0.1	40	1
STD	404.2		41.9	17	28	22.6	327	330	<10	497.3	22.41	5.78	8.8	428	7

are characterized by significant Cr values (Table 1 in the Annex; Megremi, 2010; Economou-Eliopoulos et al., 2014, 2016) as compared to the Cr content (90–110 ppm) in the earth crust (Rudnick and Fountain, 1995). Soils from the cultivated region are mostly composed of quartz, calcite, serpentinite, chromite, Fe-chromite, goethite, magnetite, kaolinite, montmorillonite, illite, ilmenite, rutile, zircon and rare earth element minerals. Fine pyrite, which is commonly framboidal is also present (Fig. 2f). Chromium in soils is hosted in chromite grains or fragments, Cr-bearing goethite and silicates transported as residual components inherited from both ophiolitic parent rocks and Ni-laterite deposits, as suggested by highly positive correlations of Cr with Ni, Co, Mn, V and Ti (Economou-Eliopoulos et al., 2012).

In the Kastoria laterite ore Mn-Fe hydrous oxides mixed with silicates (commonly Fe-serpentine) (Fig. 3), chromite grains, quartz, carbonates (calcite, siderite), Mn (hydr)oxides (pyrolusite, lithiophorite and asbolane) are dominant components, zircon and apatite are minor minerals, and organic matter is higher (5.4–10.2 wt%) than that in Central Evia laterites (1–2.0 wt%) (Megremi, 2010).

Furthermore, investigation of Fe-Ni-laterites by SEM-EDS indicated that goethite, occurring as rounded fragments from a previous stage, as well as in the matrix, is a dominant component in both laterites from Central Evia and Kastoria. However, there are significant differences in their mineral chemistry: Goethite in the Kastoria laterites showed higher Cr and Mn contents and negligible Ti content compared to that in laterite ores from Central Evia (Table 2). Also, several stages in goethite formation can be distinguished in the Kastoria ore, such as (a) high-Fe/light grey goethite of a previous stage occurring as rounded fragments in the matrix (Fig. 3d–f), (b) goethite in the matrix, with varying grey colour, which is cross-catted by fine aggregates of hematite, and dark-grey goethite (Fe-depleted) along very fine aligned elongate hematite (arrows on Fig. 3d,f) resembling bacterial cell coated by Fe-oxides. A subsequent stage of high-Mn siderite occurs cross-cutting all previous Fe (hydr)oxides (Fig. 3e). In addition, the compositional range of the chromite fragments is restricted only into the field of high-Cr type and there is an abundance of quartz in the Kastoria ores, whilst there is a wide range from high-Cr to high-Al type in the Evia laterites (Fig. 4).

5. Contamination of water

Groundwater from domestic and irrigation wells throughout central Evia (Messapia) is mostly extracted from the shallow aquifer (11–100 m). The samples from the Neogene aquifers exhibit

Table 6
Chromium concentrations and δ53Cr values for water and water leachates.

Location	Depth of well	Cr(VI)	δ53Cr
Greece			
Groundwater			
Evia			
E7	35	250	0.98
E18	20	42	1.42
E2	22	73	0.84
E5	11	117	1.22
E10	20	47	1.98
E13	18	64	1.41
MSW8	27	63	1.76
M3W8	30	40	1.34
AVLO13W (Assopos)	120	53	0.98
AVLOW8 (Assopos)	80	86	1.03
As.K.W. (Assopos)	70	900	1.16
Central Europe		Range	Range
Native water (n = 4)		2.3–15	0.4–1.7
Contaminated water (n = 7)		540–15,600	1.6–4.0
California			
Native water (n = 25)		1.2–38	0.1–3.2
Contaminated water (n = 20)		286–5760	1.2
Seawater (n = 9)		0.1–0.55	0.53–1.51
Leachates		Range	Range
rocks (RL), n = 3		38–66	0.56–0.96
Soils (SL), n = 3		40–76	0.33–0.59
Fe-Ni-laterites			
Evia, n = 2		0.6–2.0	1.01
Kastoria			
Kast 4		750	0.03
Kast7		1200	−0.21

Data for: (a) Greece from Economou-Eliopoulos (2014, 2016); (b) Central Europe from Novak et al. (2014); (c) California from Izbicki et al. (2012); (d) Seawater from Bonnand et al. (2013); Frei et al. (2014a,b), Scheiderich et al. (2015).

concentrations over the maximum acceptable level for Cr_{total} in drinking water (50 μg/L). Chromate oxyanions such as CrO_4^{2-}, $HCrO_4^-$ and $Cr_2O_7^{2-}$ cause serious health problems (ATSDR, 2000). A wide variation in Cr concentrations is found in central Evia, ranging from <2 to 360 μg/L (Table 3, Annex), in contrast to the Cr (VI) concentrations in deep (>200 m) karst-type wells in Central Evia, which are negligible (Megremi et al., 2013). An investigation of the Cr(VI) variation in groundwater wells during the dry and wet seasons recorded relatively small differences (Megremi, 2010). The high values of salinization, as exemplified by seawater elements (B, Na, Mg, Li, Se), suggest a major contribution from seawater into the groundwater aquifer in Central Evia (Table 5, Annex), which is comparable with that in the Assopos Basin (Giannoulopoulos, 2008). There is a negative trend between the Cr concentrations in water wells and the depth of the wells in Evia (Fig. 5). More specifically, the irrigation wells, hosted mostly in deeper ultramafic rocks (peridotites), exhibit lower Cr concentrations compared to those located at shallower depths within alluvial (unconfined) sediments. Groundwater from karst-type wells is characterized by negligible Cr concentrations (lower than 2 μg/L).

6. Chromium and other trace element concentrations in leachates

In general, the Cr concentrations in leachates from peridotites are much lower than those in soils, while the highest concentrations of Cr in rock leachates were measured in highly serpentinized samples with abundant calcite (Fig. 2; Table 5, Annex).

The correlation between Cr concentrations and Ca/Mg ratios is positive ($R^2 = 0.647$) for rock leachates whereas this correlation is negative ($R^2 = -0.694$) for soil leachates (Fig. 6a,c). In contrast, the correlation between Cr concentrations and Mg/Si ratios is negative ($R^2 = -0.467$) for rock leachates, while this ratio does not exhibit any clear ($R^2 = 0.017$) correlation *vs* Cr concentrations for soil leachates and groundwater (Fig. 6d and e).

Also, there is a positive correlation ($R^2 = 0.39$) between Mn and Fe *versus* Cr concentrations in rock and soil leachates (Fig. 7a and b), while Cr concentrations exhibit a negative correlation ($R^2 = -0.513$) with Ca in soil leachates and a positive correlation ($R^2 = 0.39$) in rock leachates (Fig. 7c). Chromium concentrations in rock leachates show a positive correlation ($R^2 = 0.39$) with Ca content (Fig. 7d) and a negative correlation ($R^2 = -0.54$) with Mg content (Fig. 7f). Finally, Ca concentrations in and soil leachates are positively ($R^2 = 0.69$) correlated with the Ca content in soil samples (Fig. 7e).

7. A compilation of chromium stable isotopes in natural waters and water leachates

Variations in $\delta^{53}Cr$ values, ranging from 0.84 to 1.98‰ in groundwater samples from Evia, from 0.98 to 1.16‰ in samples from the Assopos Basin and from 0.6 to 1.99‰ in samples from the Thiva Basin, have been recorded (Economou-Eliopoulos et al., 2014; 2016; Frei et al., 2014a,b). The water samples with the highest Cr(VI) concentrations (230 μg/L) from shallow wells in Central Evia Basin and (900 μg/L) in the Assopos Basin correspond to $\delta^{53}Cr$ values of 0.98‰ and 1.16‰, respectively (Table 6).

The $\delta^{53}Cr$ values measured in natural water leachates of Fe-Ni-laterites from Kastoria range between +0.03 ± 0.06‰ and −0.21 ± 0.08‰, which are much lower than the positively fractionated value (+1.01 ± 0.05‰) for the laterite leachates from Central Evia (Table 6; Fig. 8). However, many of the Evia leachates contained very low Cr concentrations, and $\delta^{53}Cr$ values could not adequately be measured (Economou-Eliopoulos et al., 2016). Chromium stable isotope values in leachates from highly serpentinized peridotites have shown a relatively small range of $\delta^{53}Cr$ values (+0.56 to +0.96‰), as have those for the soil leachates (+0.51 to +0.59‰) (Economou-Eliopoulos et al., 2014, Fig. 8).

In general, there is a positive correlation ($R^2 = 0.514$) between the $\delta^{53}Cr$ values and the depth of wells (Fig. 9).

The $\delta^{53}Cr$ measurements (+1.13 and + 0.55‰) of surface seawater from the Mediterranean Sea (Evoic Gulf), selected from a location far away from the heavily Cr(VI)-contaminated point source of the Assopos River estuary, are comparable to those for surface seawater sampled at the Assopos River estuary (+0.79 ± 0.14‰) (Table 6). These $\delta^{53}Cr$ values fall within the range published for global oceans, as exemplified by waters from Southampton and the Argentine Sea (Bonnand et al., 2013), the Parana estuary (Frei et al., 2014a,b), Oregon, Osil and the Arctic Ocean (Scheiderich et al., 2015) and elsewhere (Campbell and Yeats, 1981; Cranston, 1983; Jeandel and Minster, 1987; Mugo, 1997; Sirinawin et al., 2000).

There is a negative correlation between the $\delta^{53}Cr$ values and Cr(VI) concentrations in seawaters ($R^2 = -0.625$), in natural waters ($R^2 = -0.384$), in contaminated waters from Central Europe ($R^2 = -0.565$), and California ($R^2 = -0.636$) (Table 6; Fig. 10). The plot of $\delta^{53}Cr$ values and Cr(VI) concentrations for contaminated waters from Messapia (Central Evia) and Assopos Basin showed that they fall within fields defined by global data on contaminated water, due to natural processes and industrial activities (Fig. 10).

8. Discussion

The assessment of the sources of Cr(VI) in groundwater is a complicated subject. The present study focusses on geochemical constraints concerning the contamination source(s) by Cr(VI) in Central Evia, through an integrated set of approaches and comparison with literature data on groundwater. It is noticeable that

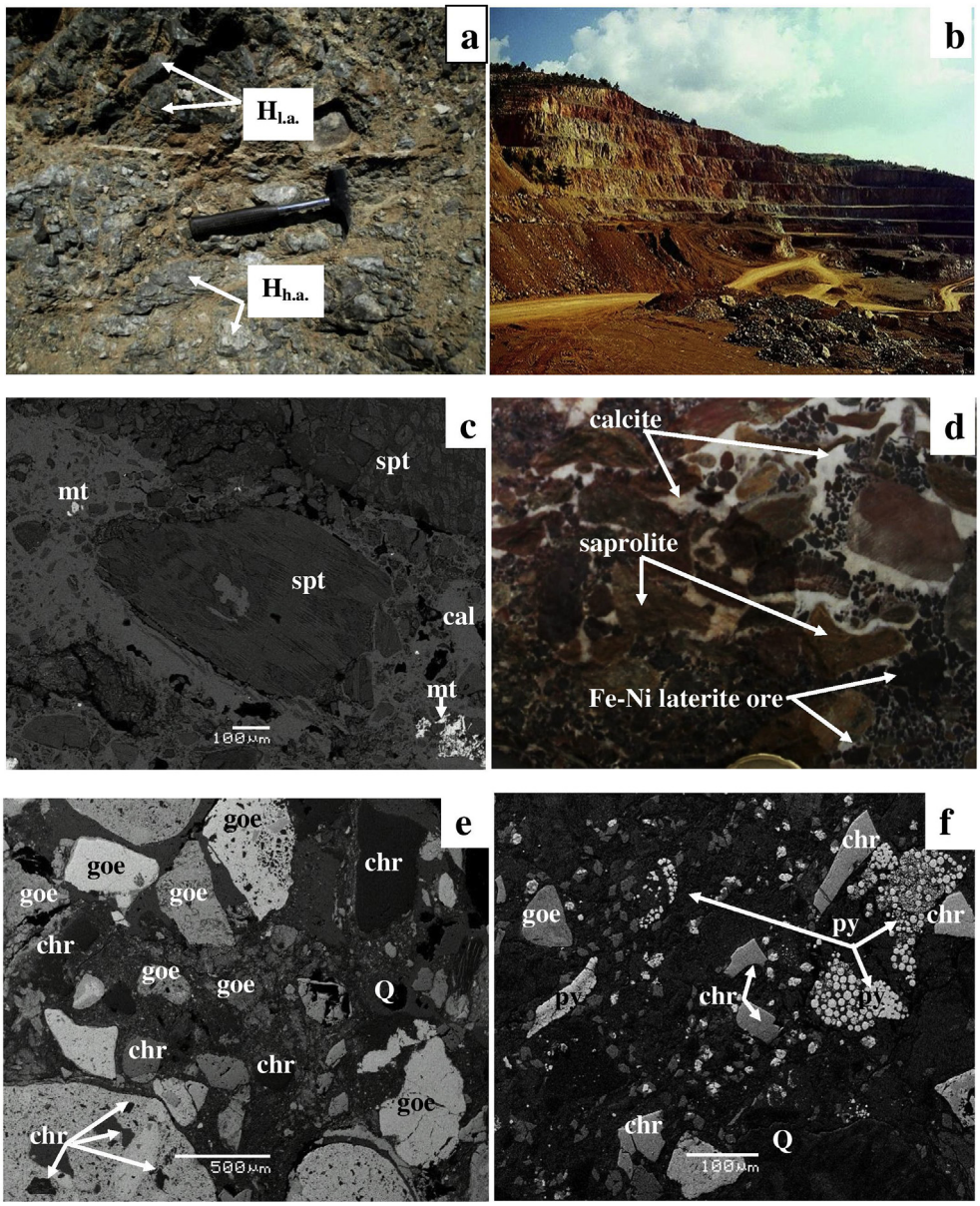

Fig. 2. Photos of ultramafic rock (2a) and Fe-Ni laterite mine from Central Evia (2b,d), showing a conglomerate, composed mostly of rounded-elongated saprolite and silicified saprolite blocks within a matrix of pisolitic laterite and calcite, and back-scattered electron images from peridotite (2c) and, Fe-Ni laterite ore (2e,f). Symbols:$H_{l.a.}$ = low altered harzburgite; $H_{h.a.}$ = highly altered harzburgite; spt = serpentine; cal = calcite; mt = magnetite; py = pyrite; Fe-chr = ferric-chromite; goe = goethite; He = hematite; sil = silicates; chl = chlorite.

certain groundwater samples showing Cr(VI) concentrations lower than 5 μg/L contain low (5 mg/L) NO_3^- and high (4.1–7.5 mg/L) TOC (total organic carbon), in contrast to highly contaminated irrigation wells [>50 μg/L Cr(VI)] showing <1 mg/L TOC (Giannoulopoulos, 2008). In addition, the reduction of Cr(VI) by organic matter is supported by field (Qin and Wang, 2017) and laboratory experimental work applying the commercial material EDC-M (Electron Donor Compound-Metals) for testing of contaminated water treatment demonstrated the ability of the organic matter to directly reduce Cr(VI) (Moraki, 2010).

Chromium in ultramafic rocks and Ni-laterites is mainly hosted in chromite, which is thermodynamically stable, within silicate minerals and Fe-hydroxides (goethite). Such minerals are more easily weathered than chromite and are potential contributors to environmental contamination by chromium (Oze, 2003; Oze et al., 2007, 2016; Megremi et al., 2013; Rajapaksha et al., 2014; Economou-Eliopoulos et al., 2014, 2016). Furthermore, fine-grained Fe (hydr)oxides, have lower surface energies than corresponding anhydrous oxides and are unstable (Navrotsky et al., 2008), since the surfaces of nano-scale Mn-oxides provide locations for hydration and redox reactions, and their reduction is thermodynamically spontaneous (negative ΔG) at low temperature (Mugo, 1997; Birkner and Navrotsky, 2012).

The mobility of chromium through rocks and soils is dependent upon its oxidation state and in turn on a complex network of synergistic and competing processes. Major factors controlling the oxidation state are the soil redox conditions, pH, and the presence of certain other metals and organic compounds (Bartlett and James, 1979; Richard and Bourg, 1991; Banerjee and Nesbitt, 1999), while the adsorption of Cr(VI), in anionic forms such as $HCrO_4^-$ or CrO_4^{2-},

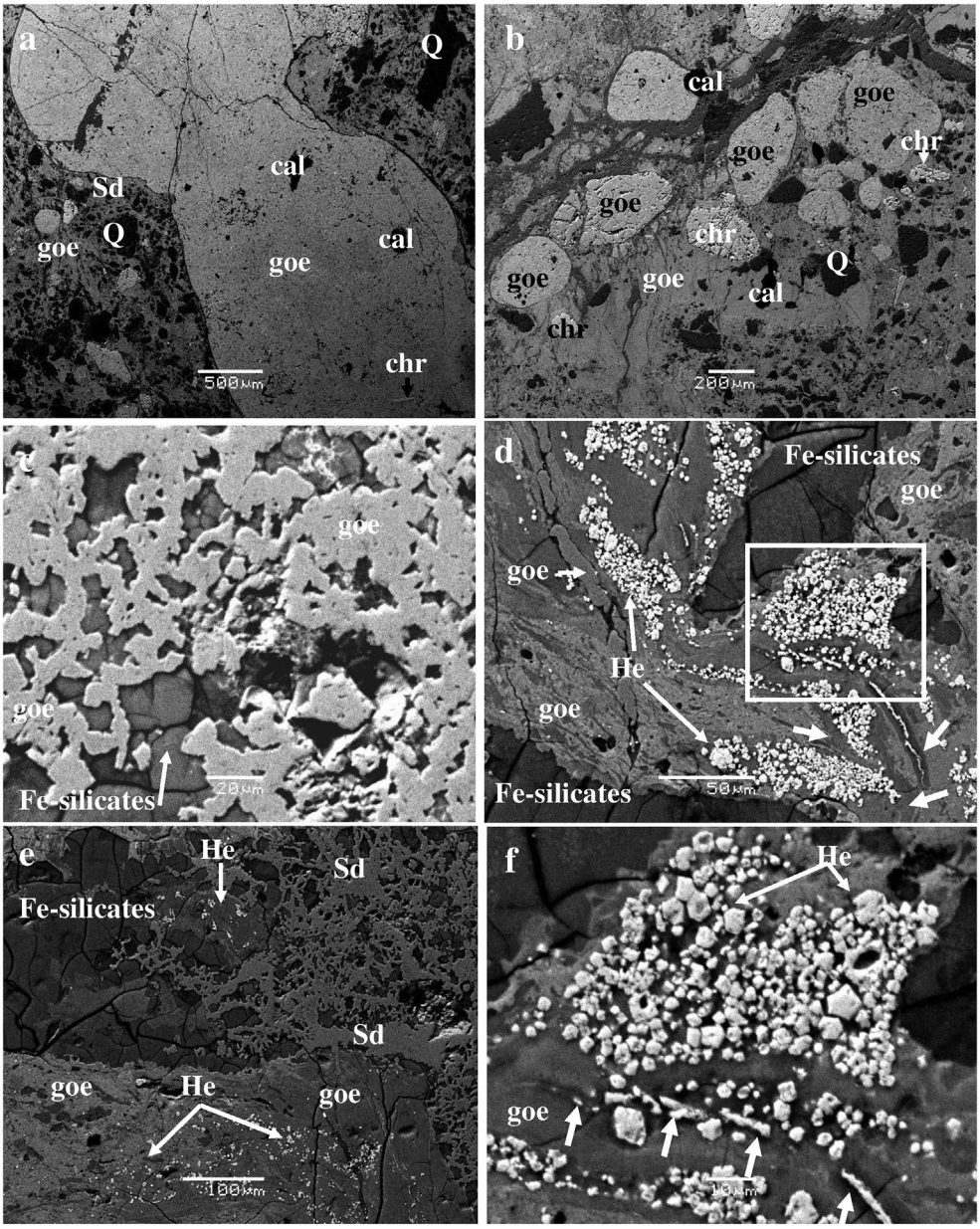

Fig. 3. Representative back-scattered SEM images from the Kastoria laterite deposit, showing light grey and dark grey goethite (3a–f), siderite (3a, e), fragments of chromite (3a, b), Very fine hematite associated with goethite and aligned elongate hematite micro-textures resembling bacterial cell coated by Fe-oxides and a dark grey zone (Fig. 3d,f; white arrows) are often. Abbreviations: goe = goethite; cal = calcite; Sd – siderite; Q = quartz; He = hematite; chr = chromite. Mineral compositions are given in Tables 2 and 3.

depends on pH (Drever, 1997). Immobilization (possibly by adsorption/co-precipitation on/with Fe-oxy-hydroxides) of Cr(III) during transport in the weathering profile (Berger and Frei, 2014) and the oxidation of Cr(III) to Cr(VI) by Mn (di)oxides (Eary and Rai, 1988a,b; Oze, 2003; Oze et al., 2007) have been well-established. Furthermore, the compilation of geological, mineralogical and geochemical data with the distribution of the δ^{53}Cr values may contribute in a better way to define the contamination source(s).

8.1. Evidence from chromium stable isotopes

8.1.1. Diversity of the δ^{53}Cr and Cr(VI) values in Ni-laterite water leachates

A diversity between Cr(VI) concentrations in the water leachates for Ni-laterites from Central Evia and Kastoria (Table 6; Fig. 10), and fractionation of the δ^{53}Cr values relative to the average bulk silicate earth δ^{53}Cr composition of about ~0.1‰ (Schoenberg et al., 2008), may imply differences in the effectiveness of the dissolution of Cr from the Ni-laterite ore during serpentinization/weathering of the parent peridotites, in transport and/or in post mobilization redox processes. Relatively high δ^{53}Cr values (0.56–0.96‰) in water leachates from highly altered peridotites (Fig. 2a) and Ni-laterites (up to 1.01‰ δ^{53}Cr) from Central Evia seem to be consistent with those determined (up to ~+1.22‰ δ^{53}Cr) in serpentinites (Farkaš et al., 2013). These authors proposed that serpentinization could shift altered peridotites to isotopically high δ^{53}Cr, and interpreted the extreme high δ^{53}Cr in serpentinites as a result of isotopic fractionation during dehydration accompanying subduction and/or addition of Cr(VI) that was fractionated on mineral surfaces prior to entering solution (Farkaš et al., 2013; Wang et al., 2016).

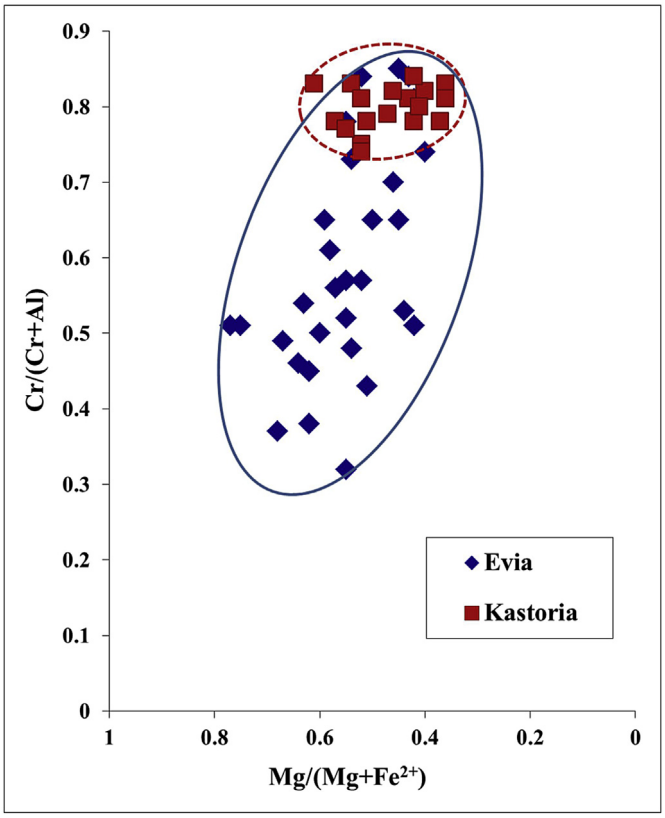

Fig. 4. Compositional variation of Cr, as Cr# [Cr/(Cr + Al)] *versus* Mg, as Mg# [Mg/(Mg + Fe2+)] of chromites in Fe-Ni-laterite deposits of Evia and Kastoria.

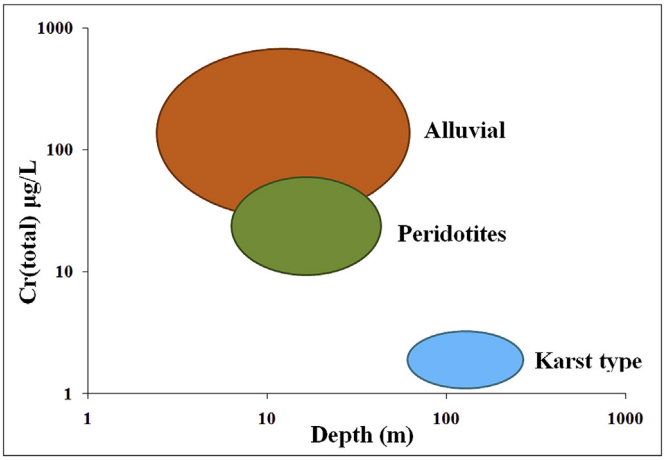

Fig. 5. Bivariate plot of wells depth from central Euboea *versus* their Cr (total) concentrations (after Megremi et al., 2013).

The complexity of redox processes during the mobilization and transport of Cr(VI) from the landmasses to the oceans has not been studied extensively. It is well known that Cr(III), by the catalytic action of MnO_2, is oxidized in soils, but the isotopic fractionation in this process is still unclear. These results support the contention that Cr isotopes fractionate during oxidative weathering on land (Frei et al., 2014a,b; Crowe et al., 2013; Frei and Polat, 2012; Paulukat et al., 2015; D'Arcy et al., 2016) and/or during transport to the oceans (Frei et al., 2009; Bonnand et al., 2013). More specifically, available seawater data (Bonnand et al., 2013; Scheiderich et al., 2015; Paulukat et al., 2015) indicate higher than bulk silicate earth δ^{53}Cr values, and mass balance modelling imply that river waters should also be characterized by heavy Cr isotopes (Frei et al., 2014a,b; D'Arcy et al., 2016). Assuming, by results hitherto published on riverine waters, that partial back-reduction of mobile Cr(VI), wither already in the soils and/or during riverine transport, must be responsible for the generally positive δ^{53}Cr values in these systems. The fate of Cr(VI) in the seawater has been addressed by Scheiderich et al. (2015), and confirmed by Paulukat et al. (2015), who argued for the mixing trend in [Cr] vs. d^{53}Cr values of modern seawater to arise from fractionation during the reduction of Cr(VI) in surface waters and oxygen minimum zones, scavenging of isotopically light Cr(III) to deeper water and sediment, and subsequent release of this seawater-derived Cr(III) back into seawater, either as organic complexes with Cr(III) or after oxidation to Cr(VI). The above scenarios also seem to be consistent with the general increasing trend defined between δ^{53}Cr values and the depth of the aquifer (Fig. 9), which potentially reflects the decrease in soluble O_2 which would be expected with increasing depth.

However, the Kastoria Fe-Ni-laterites that have experienced seawater alteration during re-deposition and significant fluid infiltration during diagenesis and post-diagenetic stages show very limited fractionation of their Cr isotopes. The presence of pyrite and the absence any zone of ferrian chromite at the peripheral parts and along cracks of chromite fragments in samples of Ni-laterites from Central Evia (Fig. 2f) as well as the presence of siderite cross-cutting earlier stages of Fe-(hydr)oxides and the Fe-depleted zones (dark grey) of goethite (Fig. 3d,f; white arrows) in the Kastoria laterites may point to reducing conditions that prevailed during diagenetic/post-diagenetic processes in both areas. Although a variety of reductants are present that could have potentially back-reduced mobilized Cr(VI), in the Kastoria Ni-laterite ores (Fig. 3) nearly unfractionated δ^{53}Cr values measured in the Kastoria leachates may indicate the existence of oxidative materials in excess, and/or the effects of additional factors on the kinetics of redox reactions. Also, the development of the Kastoria laterite deposit atop of peridotites, in contrast to those in Evia which were tectonically emplaced over a carbonate basement (Valeton et al., 1987), may indicate a significant role of the transportation flow for the enrichment of heavy Cr isotopes, which seems to be consistent with the positive trend between the δ^{53}Cr values and the depth of groundwater (Fig. 9).

8.1.2. Variation on the δ^{53}Cr vs Cr(VI) values in groundwater

Chromium(VI) concentrations in excess of the European permeable level of 50 µg/L are common in shallow alluvial aquifers in Central Evia, where ultramafic rocks and alkaline and oxic groundwater conditions are well known (Megremi, 2010) and in the Assopos Basin (Tables 4 and 6). Positive δ^{53}Cr values of 1.2 and 2.3‰ measured in groundwater having low Cr concentrations, have been attributed to the addition of Cr(VI) that was fractionated on mineral surfaces prior to entering solution and/or to the decrease of the estimated O_2 concentrations caused the reduction of Cr(VI) to Cr(III) and subsequently removed from solution (Farkaš et al., 2013; Wang et al., 2016). Thus the highest δ^{53}Cr values recorded in water from deep wells (Fig. 9), seems to be consistent with those in wells of long flow paths through alluvial aquifers (Izbicki et al., 2008).

Higher Cr(VI) concentrations and lower δ^{53}Cr values in aquifers may suggest that either reductive fractionation and removal of Cr(VI) from solution has not occurred, or origin of Cr from a different source and evolution of the δ^{53}Cr composition along a different geochemical pathway Izbicki et al. (2008). The δ^{53}Cr values around zero in the water leachates of the Ni-laterites from Kastoria (Table 6) are consistent with the suggestion that only δ^{53}Cr values are not necessarily diagnostic of anthropogenic contamination by Cr (Izbicki et al., 2008). In addition, t the near zero δ^{53}Cr

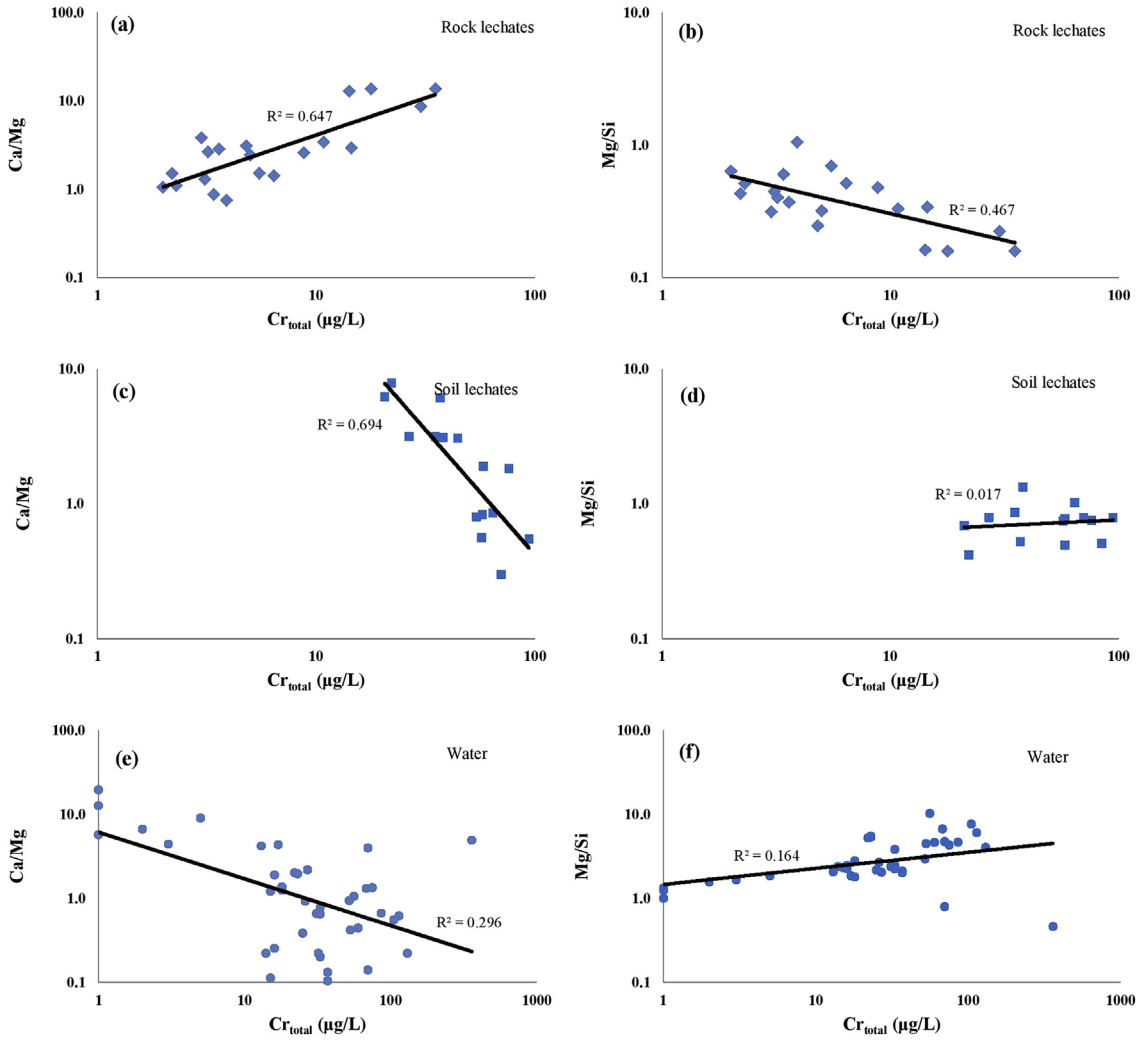

Fig. 6. Plots of the Ca/Mg and Mg/Si ratios *versus* Cr total concentrations in rock (Fig. 6a and b) and soil (Fig. 6c and d) leachates, and groundwater (Fig. 6e and f). Data from (Tables 4 and 5).

values in the water leachates of the Kastoria Ni-laterites suggesting lack of reductive fractionation and removal of Cr(VI) from solution poin to excess of oxidative reagents.

In a comparison of the variation of δ^{53}Cr values in groundwater, from Central Europe and California, indicating fractionation, and the Cr isotope compositions of worldwide seawater (Bonnand et al., 2013; Farkaš et al., 2013; Economou-Eliopoulos et al., 2014, 2016; Scheiderich et al., 2015; Lelli et al., 2014; Novak et al., 2014; Izbicki et al., 2015) it appears that the groundwater samples from the Evia and Assopos basins fall within the fields of both naturally and anthropogenically contaminated waters (Fig. 10). In particular, the data conforming to those from California (Izbicki et al., 2012), as plotted in Fig. 10, may be helpful in providing clues for the source of potential contamination.

9. Conclusions

The compilation of SEM/EDS results and literature data from a variety of perspectives, including mineralogy, geochemistry, isotopes, leaching experiments on rocks, soils and Ni-laterites from Central Evia and elsewhere, leads us to the following conclusions:

1) Although near zero δ^{53}Cr values in groundwater are commonly interpreted as the result of human activities, unfractionated (near zero) δ^{53}Cr values in leachates from Ni-laterites of Kastoria suggest that such values are not necessarily diagnostic for anthropogenic sources alone.
2) Mn-(hydr)oxides in excess of potential reductants, and the fine-grained nature of these components in the Kastoria Fe-Ni-laterite ore, may be major controlling factors for the increased release of Cr(VI) into the water leachates of the ore.
3) A positive correlation ($R^2 = 0.514$) between the δ^{53}Cr values and depth of the aquifers, may reflect the decrease in soluble O_2 with increasing depth.
4) The development of the Kastoria laterite deposit atop parent peridotites, in contrast to those in Evia tectonically emplaced atop a carbonate basement, after a long transportation flow, may support the role of a long distance transportation to explain positively fractioned δ^{53}Cr values.
5) The δ^{53}Cr values and Cr(VI) concentrations in contaminated water from the Evia and Assopos Basins, are plotted in fields defined by global database for contaminated water by both natural processes and anthropogenic activities, reflecting probably potential contamination sources.

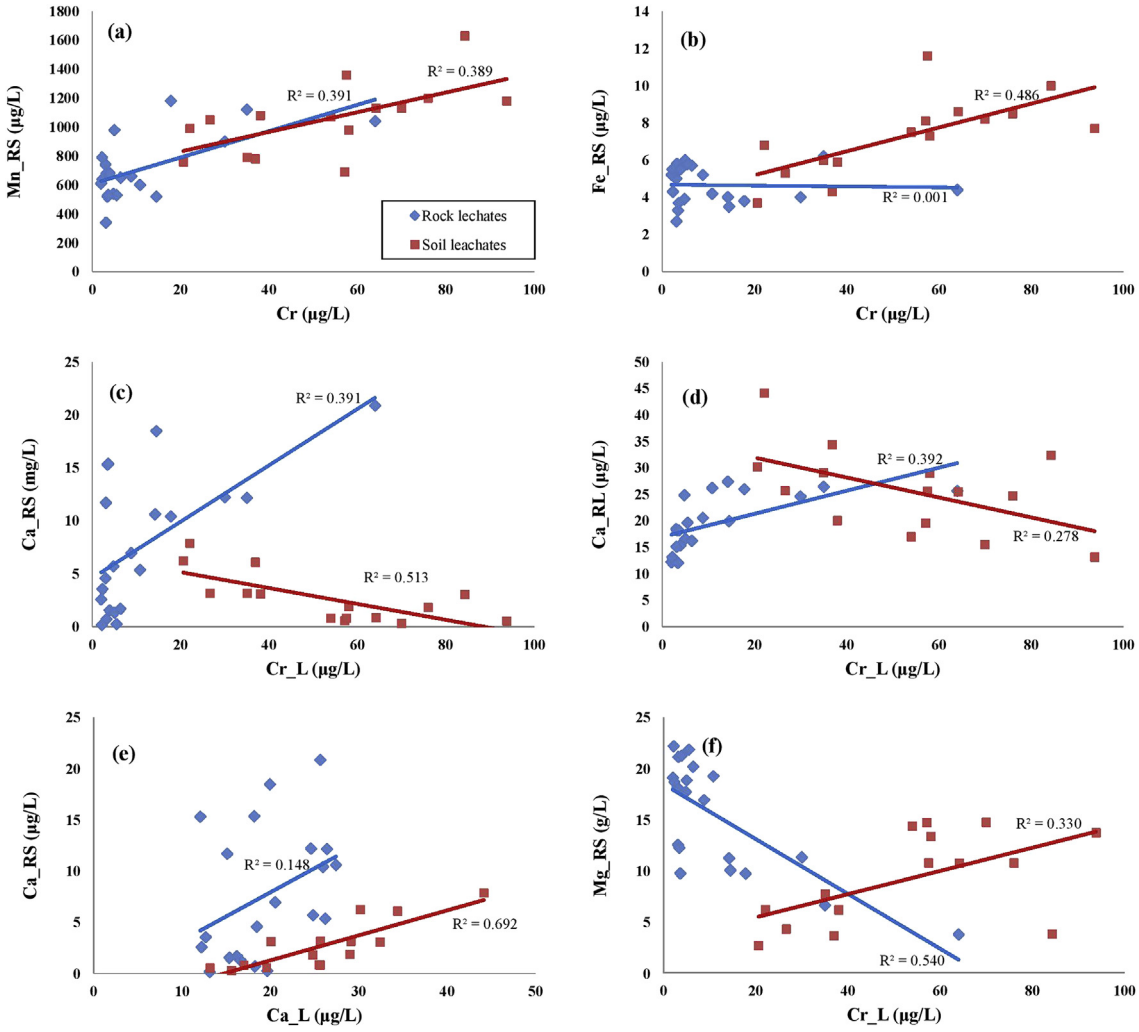

Fig. 7. Plots of the Mn, Fe, and Ca contents *versus* Cr concentrations in rock and soil leachates (Fig. 7a, b, c); Ca and Mg versus Cr (Fig. 7 d, e) concentrations in rock and soil leachates (Fig. 7d, f); Ca content I rocks and soils versus Ca concentration in leachates (Fig. 7f). Data from (Tables 1 and 5).

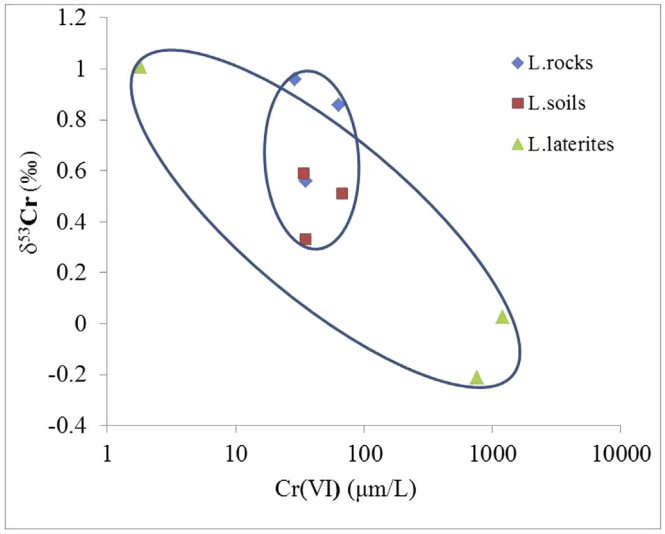

Fig. 8. Bivariate plot of δ^{53}Cr values in leachates (L) for rocks, soils and laterites from Central Evia (Data from Table 6).

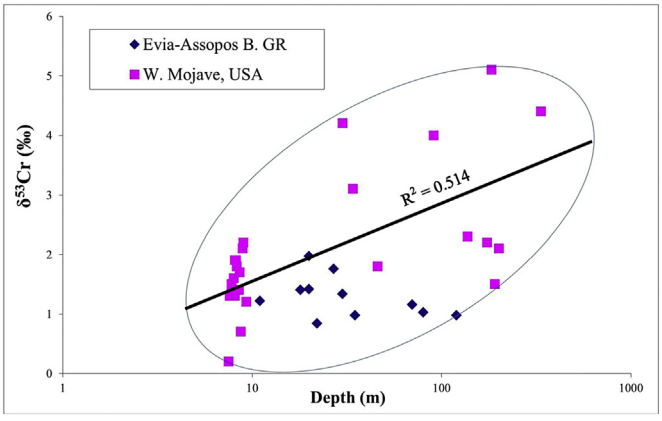

Fig. 9. Bivariate plot of wells depth from central Euboea and W, Mojave (USA) *versus* their δ^{53}Cr values in water (Data from Table 6; Izbicki et al., 2008).

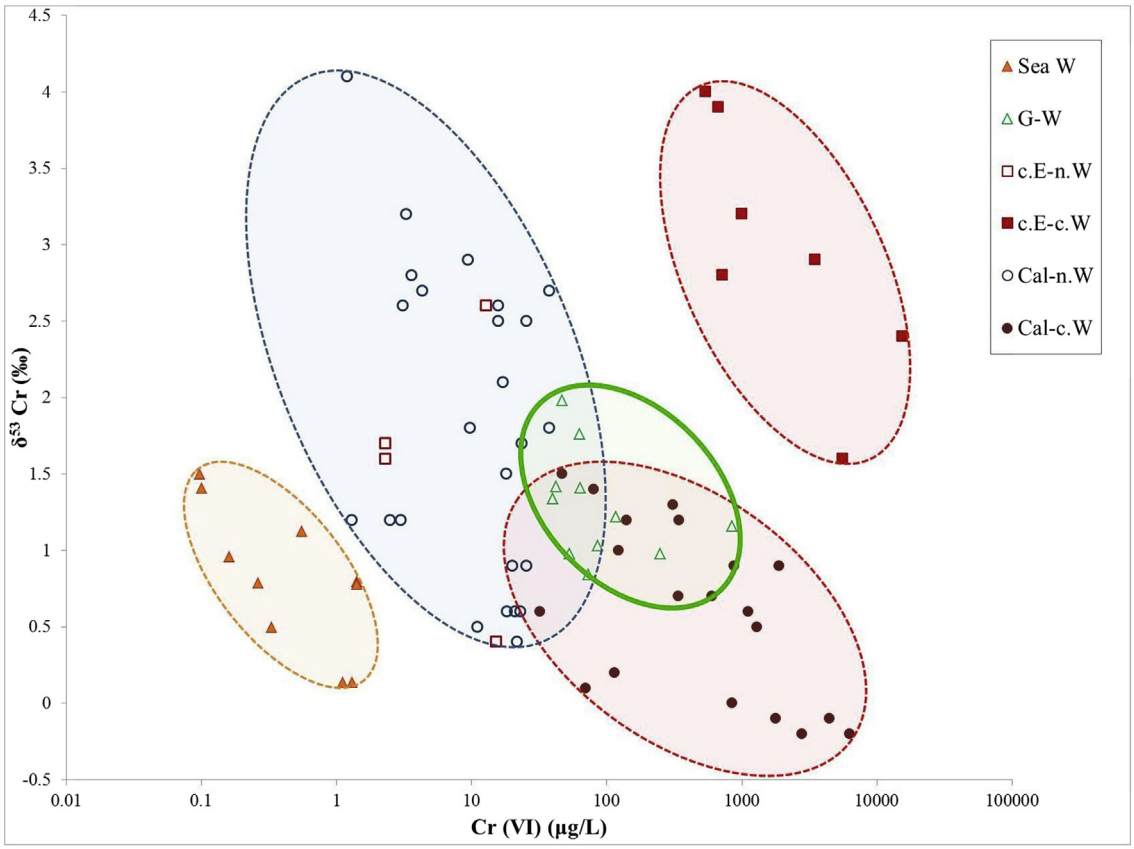

Fig. 10. Diagram of δ^{53}Cr values in Global sea water (Sea W), including two samples from the Mediterranean sea; Groundwater from Evia and Assopos Basin (G-W); groundwater from Central Europe contaminated by geogenic processes (c.E.-n.W) and anthropogenic activities (c.E.-c.W.) and California (Cal.-n.W) and (Cal.-c,W), respectively. Data from Bonnand et al. (2013); Economou-Eliopoulos et al. (2014, 2016); Lelli et al. (2014); Novak et al. (2014); Izbicki et al. (2012, 2015); Paulukat et al. (2015); Scheiderich et al. (2015).

6) Variation in δ^{53}Cr values *versus* Cr(VI) concentrations in water from a global database, compiled with geological, mineralogical and geochemical data, may provide a basis for the discrimination of potential contamination sources.

Acknowledgments

The Mayor and the Municipality of Messapia-Dirfis is acknowledged for the financial support of this work (A.K. 70/3/11730). Financial support through the Danish Agency for Science, Technology and Innovation grant number 11-103378 to RF is highly appreciated. We would like to thank Toby Leeper for always maintaining the mass spectrometer in optimal running conditions, and Toni Larsen for help in separation of Cr from the samples. Many thanks are expressed to Prof. Dr. Michael Kersten, Executive Editor and the anonymous reviewers for their constructive criticism and suggestions that improved the manuscript.

References

Alevizos, G., 1997. Mineralogy, Geochemistry and Origin of the Sedimentary Fe–Ni Ores of Lokris. Ph.D. Unpublished thesis. Technical University. Crete (245 pp). (in Greek with English abstract).

ATSDR (Agency for Toxic Substances, Disease Registry), 2000. Toxicological Profile for Chromium. Agency for Toxic Substances and Disease Registry. Public Health Service, U.S. Department of Health and Human Services, 2000. http://www.atsdr.cdc.gov/toxprofiles/tp7.html.

ATSDR, 2014. Standard Test Method for Collection and Analysis of Hexavalent Chromium in Ambient Atmospheres (Withdrawn 2014).

Ball, J.W., Izbicki, J.A., 2004. Occurrence of hexavalent chromium in ground water in the western Mojave Desert, California. Appl. Geochem 19, 1123–1135.

Banerjee, D., Nesbitt, H.W., 1999. Oxidation of aqueous Cr(III) at birnessite surfaces: constraints on reaction mechanism. Geochim. Cosmochim. Acta 63 (11–12), 1671–1687.

Bartlett, R.J., James, B., 1979. Behavior of chromium in soils: III. Oxid. J. Environ. Qual. 8, 31–35. http://dx.doi.org/10.2134/jeq1979.00472425000800010008x.

Becquer, T., Quantin, C., Sicot, M., Boudot, J.P., 2003. Chromium availability in ultramafic soils from New Caledonia. Sci. Total Environ. 30, 251–261.

Berger, A., Frei, R., 2014. The fate of chromium during tropical weathering: a laterite profilefrom Central Madagascar. Geoderma 213, 521–532.

Birkner, N., Navrotsky, A., 2012. Thermodynamics of manganese oxides: effects of particle size and hydration on oxidation-reduction equilibria among hausmannite, bixbyite, and pyrolusite. Am. Mineralogist 97, 1291–1298.

Bonnand, P., James, R.H., Parkinson, I.J., Connelly, D.P., Fairchild, I.J., 2013. The chromium isotopic composition of seawater and marine carbonates. Earth Planet. Sci. Lett. 382, 10–20.

Burland and Edwards. 1999 Campbell, J.A., Yeats, P.A., 1981. Dissolved chromium in the northwest Atlantic Ocean. Earth Planet. Sci. Lett. 53, 427–433.

Cranston, R.E., 1983. Chromium in Cascadia Basin, northeast Pacific Ocean. Mar. Chem. 13, 109–125.

Crowe, S.A., Døssing, L.N., Beukes, N.J., Bau, M., Kruger, S.J., Frei, R., Canfield, D.E., 2013. Atmospheric oxygenation 3 billion years ago. Nature 501, 535–538.

D'Arcy, J., Babechuk, M.G., Døssing, L.N., Frei, R., Gaucher, C., 2016. Processes controlling the chromium isotopic composition of river water: Constrains from basaltic river catchments. Geochim. Cosmochim. Acta 186, 296–315.

Dermatas, D., Mpouras, T., Chrysochoou, M., Panagiotakis, I., Vatseris, C., Linardos, N., Sakellariou, L., 2015. Origin and concentration profile of chromium in a Greek aquifer. J. Hazard. Mater. 281, 35–46.

Dimitroula, H., Syranidou, E., Manousaki, E., Nikolaidis, N.P., Karatzas, G.P., Kalogerakis, N., 2015. Mitigation measures for chromium-VI contaminated groundwater - The role of endophytic bacteria in rhizofiltration. J. Hazard. Mater. 281, 114–120. http://dx.doi.org/10.1016/j.jhazmat.2014.08.005 ([PubMed] [Cross Ref]).

Dokou, Z., Karagirorgi, V., Karatzas, G.P., Nikolaidis, N.P., Kalogerakis, N., 2015. Large scale groundwater flow and hexavalent chromium transport modeling under current and future climatic conditions: The case of Asopos River Basin. Environ. Sci. Pollut. Res. http://dx.doi.org/10.1007/s11356-015-5771-1.

Drever, J.I., 1997. The Geochemistry of Natural Waters, Surface and Groundwater Environments, third ed. Prentice Hall, Upper Saddle River, NJ.

Eary, L.E., Rai, D., 1988a. Chromate removal from aqueous wastes by reduction with

ferrous ion. Environ. Sci. Technol. 22, 972–977.
Eary, L.E., Rai, D., 1988b. Kinetics of chromate reduction by ferrous ions derived from hematite and biotite at 25 °C. Amer. I, Sci. 1989 (289), 180–213.
Economou-Eliopoulos, M., Antivach, D., Vasilatos, Ch, Megremi, I., 2012. Evaluation of the Cr(VI) and other toxic element contamination and their potential sources: The case of the Thiva basin (Greece). Geosci. Front. 1–17.
Economou-Eliopoulos, M., Megremi, I., Vasilatos, Ch, 2011. Factors controlling the heterogeneous distribution of Cr(VI) in soil, plants and groundwater: evidence from the Assopos basin, Greece. Chem. Erde 71, 39–52.
Economou-Eliopoulos, M., Megremi, I., Atsarou, K., Theodoratou, Ch, Vasilatos, Ch, 2013. Spatial evolution of the chromium contamination in soils from the Assopos to Thiva basin and C. Evia (Greece) and potential source(s): Anthropogenic versus natural processes. Geosciences 3, 140–158.
Economou-Eliopoulos, M., Frei, R., Atsarou, C., 2014. Application of chromium stable isotopes to the evaluation of Cr (VI) contamination in groundwater and rock leachates from central Euboea and the Assopos basin (Greece). Catena 122, 216–228.
Economou-Eliopoulos, M., Frei, R., Megremi, I., 2016. Potential leaching of Cr(VI) from laterite mines and residues of metallurgical products (red mud and slag): An integrated approach. J. Geochem. Explor. 262, 40–49. www.elsevier.com/locate/gexplo.
Eliopoulos, D., Economou-Eliopoulos, M., 2000. Geochemical and mineralogical characteristics of Fe–Ni and bauxitic–laterite deposits of Greece. Ore Geol. Rev. 16, 41–58.
Eliopoulos, D.G., Economou-Eliopoulos, M., Apostolikas, A., Golightly, J.P., 2012. Geochemical features of nickel–laterite deposits from the Balkan Peninsula and Gordes, Turkey: the genetic and environmental significance of arsenic. Ore Geol. Rev. 48, 413–427.
Fantoni, D., Brozzo, G., Canepa, M., Cipolli, F., 2002. Natural hexavalent chromium in groundwaters interacting with ophiolitic rocks. Environ. Geol. 42, 871–882.
Farkaš, J., Chrastny, V., Novak, M., Cadkova, E., Pasava, J., Chakrabarti, R., Jacobsen, S.B., Ackerman, L., Bullen, T.D., 2013. Chromium isotope variations (delta Cr-53/52) in mantle-derived sources and their weathering products: implications for environmental studies and the evolution of delta Cr-53/52 in the Earth's mantle over geologic time. Geochim. Cosmochim. Acta 123, 74–92.
Frei, R., Gaucher, C., Poulton, S.W., Canfield, D.E., 2009. Fluctuations in Precambrianatmospheric oxygenation recorded by chromium isotopes. Nature 461, 250–253.
Frei, R., Poiré, D., Frei, K.M., 2014a. Weathering on land and transport of chromium to the ocean in a subtropical region (Misiones, NW Argentina): a chromium stable isotope perspective. Chem. Geol. 381, 110–124.
Frei, R., Polat, A., 2012. Chromium Isotope Fractionation during Oxidative Weathering - Implications from the Study of a Paleoproterozoic (Ca. 1.9 Ga) Paleosol, Schreiber Beach, vol. 224. Precambrian Research, Ontario, Canada, pp. 434–453.
Frei, R., Frei, K.M., Economou-Eliopoulos, M., Atsarou, C. and Koilakos, D., 2014b. Application of Chromium Stable Isotopes to the Evaluation of Cr (VI) Contamination in Groundwater and Rock Leachates from Central Euboea, the Assopos Basin and Thebes Valley (Greece). AGU Fall Meeting, Colorado, Abstracts 1, 0926.
Giannoulopoulos, P., 2008. Hydrogeological–hydro–chemical Survey of Groundwater Quality in the Wider Area of Asopos River Basin, Viotia Prefecture. Institute of Geology and Mineral Exploration (IGME), Athens (in Greek).
Gkoutzioupa, K., Alevizos, G., Stratakis, A., Petrakis, E., Apostolikas, A., 2016. Quality Characteristics and Washability Treatment of Nickeliferous Iron Ore of Agios Athanasios Deposit (Kastoria, Greece). Geomaterials 6, 39–49. http://dx.doi.org/10.4236/gm.2016.62004.
Izbicki, J.A., Ball, J.W., Bullen, T.D., Sutley, S.J., 2008. Chromium, chromium isotopes and selected trace elements, western Mojave Desert, USA. Appl. Geochem. 23 (5), 1325–1352.
Izbicki, J.A., Bullen, T.D., Martin, P., Schroth, B., 2012. Delta chromium-53/52 isotopiccomposition of native and contaminated groundwater, Mojave Desert, USA. Appl. Geochem. 27 (4), 841–853.
Izbicki, J.A., Wright, M.T., Seymour, W.A., McCleskey, R.B., Fram, M.S., Belitz, K., Esser, B.K., 2015. Cr(VI) occurrence and geochemistry in water from public-supply wells in California. Appl. Geochem. 63, 203–217.
Jeandel, C., Minster, J.F., 1987. Chromium behavior in the ocean: Global versus regional processes. Glob. Biogeochem. Cycles 1, 131–154.
Kabata-Pendias, A., 2000. Trace Elements in Soils and Plants. CRC Press, Inc, Boca Raton, Florida, p. 550.
Kalatha, S., Economou-Eliopoulos, M., 2015. Framboidal pyrite and bacterio morphic goethite at transitional zones between Fe–Ni-laterites and limestones: Evidence from Lokris, Greece. Ore Geol. Rev. 65, 413–425.
Katsikatsos, G., Fytrolakis, N., Perdikatsis, V., 1980. Contribution to the genesis of lateritic depositsoftheupperCretaceoustransgressioninAtticaandcentralEuboea(Greece). Proceedings of International Symposium in Metallogeny of Mafic and Ultramafic Complexes. The Eastern Mediterranean–Western Asia Area and its Comparison With Similar metallogenic Environments in the World, Athens 1980,. 257–265.
Kazakis, N., Kantiranis, N., Kalaitzidou, K., Kaprara, E., Mitrakas, M., Frei, F., Vargemezis, G., Tsourlos, P., Zouboulis, A., Filippidis, A., 2017. Origin of hexavalent chromiumin groundwater: The example of Sarigkiol Basin, Northern Greece. Sci. Total Environ. 593–594, 552–566.
Lelli, L., Kokhanovsky, A.A., Rozanov, V.V., Vountas, M., Burrows, J.P., 2014. Linear trends in cloud top height from passive observations in the oxygen A-band. Atmos. Chem. Phys. 14, 5679–5692. http://dx.doi.org/10.5194/acp-14-5679-2014.
Losi, E., Amrhein, C., Frankenberger, W.T.J., 1994. Environmental biochemistry of chromium. Rev. Environ. Contam. Toxicol. 136, 91–131.
Megremi, I., 2009. Distribution and bioavailability of Cr in Central Evia. Greece. Cent. Eur.J. Geosci. 2, 103–123.
Megremi, I., 2010. Controlling Factors of the Mobility and Bioavailability of Cr and Other Metals at the Environment of Ni-laterites. Ph.D thesis. Univ. of Athens, p. 316.
Megremi, I., Vasilatos, Ch, Atsarou, A., Theodoratou, Ch, Economou-Eliopoulos, M., Mitsis, I., 2013. Geochemical evidences for the sources of the Cr(VI) contamination in groundwater in central Euboea and Assopos-Thiva basins, Greece. Natural versus Anthropogenic Origin. Eur. Water 41, 23–34.
Moraki, A., 2010. Assessment of groundwater contamination by hexavalent chromium and its remediation at Avlida area, Central Greece. Hell. J. Geosci. 45, 175–183.
Mugo, F.W., 1997. Factors Contributing Woodfuel Scarcity and the Consequent Use of Crop Residues for Domestic Energy in Rural Kenya (A thesis presented to the Faculty of the Graduate School of Cornell University in partial fulfillment of the requirements for the degree of Master of Science. Ithaca, NY. USA).
Novak, M., Chrastny, V., Cadkova, E., Farkas, J., Bullen, ThD., Tylcer, J., Szurmanova, Z., Cron, M., Prechova, E., Curik, J., Stepanova, M., Pasava, J., Erbanova, L., Houskova, M., Puncochar, K., Hellerich, L.A., 2014. Common occurrence of a positive δ^{53}Cr shift in Central European waters contaminated by geogenic/industrial chromium relative to source values. Environ. Sci. Technol. 48 (11), 6089–6096.
Navrotsky, A., Mazeina, L., Majzlan, J., 2008. Size-driven structural and thermodynamic complexity in iron oxides. Science 319, 1635–1638.
Oze, C., 2003. Chromium Geochemistry of Serpentinites and Serpentine Soils. Dissertation. Department of Geological and Environmental Sciences, Stanford University.
Oze, C., Bird, K.D., Fendorf, S., 2007. Genesis of hexavalent chromium from natural sources in soil and groundwater. PNAS 104, 6544–6549.
Oze, C., Fendorf, S., Bird, K.D., Coleman, G.R., 2004. Chromium geochemistry of serpentine soils. Int. Geol. Rev. 46, 97–126.
Oze, C., Sleep, N.H., Coleman, R.G., Fendorf, S., 2016. Anoxic oxidation of chromium. Geology 44, 543–546.
Paulukat, C., Dossing, L.N., Mondal, S.K., Voegelin, A.R., Frei, R., 2015. Oxidative release of chromium from the Archean ultramafic rocks, its transport and environmental impact – a Cr isotope perspective on the Sukinda valley ore district (Otissa, India). Appl. Geochem 59, 125–138.
Qin, L., Wang, X., 2017. Chromium isotope geochemistry. Rev. Mineral. Geochem. 82, 379–414.
Rajapaksha, A.U., Vithanage, M., Oze, C., Bandara, W.M.A.T., Weerasooriya, R., 2014. Nickelandmanganese release in serpentine soil fromthe Ussangoda ultramafic complex, SriLanka. Geoderma 189–190.
Richard, F.C., Bourg, A.C.M., 1991. Aqueous geochemistry of chromium: a review. Water Res. 25, 807–816.
Rudnick, R.L., Fountain, D.M., 1995. Nature and composition of the continental crust: a lower crustal perspective. Rev. Geophys 33, 267–309.
Salunkhe, P.B., Dhakephalkar, P.K., Paknikar, K.M., 1998. Bioremediation of hexavalent Cr in soil microcosms. Biotechnol. Lett. 20, 749–751.
Scheiderich, K., Amini, M., Holmden, C., Francois, R., 2015. Global variability of chromium isotopes in seawater demonstrated by Pacific, Atlantic, and Arctic Ocean samples. Earth Planet. Sci. Lett. 423, 87–97.
Schiller, M., Van Kooten, E., Holst, J.C., Olsen, M.B., Bizzarro, M., 2014. Precise measurement of chromium isotopes by MC–ICPMS. J. Anal. Atomic Spectrom. 29, 1406–1416.
Schoenberg, R., Zink, S., Staubwasser, M., von Blanckenburg, F., 2008. The stable Cr isotope inventory of solid Earth Reservoirs determined by double-spike MC-ICP-MS. Chem. Geol. 249, 294–306.
Sirinawin, W., Turner, D.R., Westerlund, S., 2000. Chromium (VI) distributions in the Arctic and the Atlantic Oceans and a reassessment of the oceanic Cr cycle. Mar. Chem. 71 (3–4), 265–282.
Skarpelis, N., 1997. Eocene nickel laterite deposits in Greece and Albania, 1997. In: Papunen, H. (Ed.), Miner. Deposits: Res. Explor., where Do They Meet? Balkema, Rotterdam, pp. 503–506.
Skarpelis, N., Laskou, M., Alevizos, G., 1993. Mineralogy and geochemistry of the nickeliferous lateritic iron-ores of Kastoria. N.W. Greece. Chem. Erde 53, 331–339.
Tziritis, E.P., 2009. Assessment of NO^{3-} contamination in a karstic aquifer, with the use of geochemical data and spatial analysis. Environ. Earth Sci. 60, 1381–1390.
Valeton, I., Biermann, M., Reche, R., Rosenberg, F., 1987. Genesis of Ni-laterites and bauxites in Greece during the Jurassic and Cretaceous, and their relation to ultrabasic parent rocks. Ore Geol. Rev. 2, 359–404.
Vasilatos, Ch, Megremi, I., Economou-Eliopoulos, M., Mitsis, I., 2008. Hexavalent chromium and other toxic elements in natural waters in the Thiva – Tanagra – Malakasa Basin, Greece. Hellenic J. Geosciences 43, 57–66.
Wang, X., Reinhard, C., Planavsky, N., Owens, J.D., Lyons, T., Johnson, C.M., 2016. Sedimentary chromium isotopic compositions across the Cretaceous OAE2 at Demerara Rise Site 1258. Chem. Geol. 429, 85–92.